



Paper 5: 1.5

**X-RAY VISUALISATION AND DISSOLVED GAS  
QUANTIFICATION:  
MULTIPHASE FLOW RESEARCH AND  
DEVELOPMENT AT NEL**

**Authors:**

**Andrew R.W. Hall and Anne E. Corlett, NEL, U.K.**

**Organiser:**

**Norwegian Society of Chartered Engineers  
Norwegian Society for Oil and Gas Measurement**

**Co-organiser:**

**National Engineering Laboratory, UK**

**Reprints are prohibited unless permission from the authors  
and the organisers**

# X-RAY VISUALISATION AND DISSOLVED GAS QUANTIFICATION: MULTIPHASE FLOW RESEARCH AND DEVELOPMENT AT NEL

Andrew R.W. Hall & Anne E. Corlett  
National Engineering Laboratory, UK

## SUMMARY

NEL is actively investigating new techniques for the measurement of multiphase flows. This paper describes two such investigations, an X-ray system to visualise three-phase flows and a manometric/volumetric system to quantify the dissolved gas content of oil/gas flows.

The X-ray system was used in both horizontal and vertical flows, covering slug, annular and bubble flow regimes. Also covered were stratified (horizontal only) and churn (vertical only) flows. The system was able to provide visualisation of features not visible in flows with low water cut (due to poor light transmission through oil) and therefore increased the understanding of three-phase flow behaviour.

Quantifying the amount of dissolved gas within a hydrocarbon oil is of importance to the oil industry due to the problems associated with the artificial decrease in density of a gas filled oil and the effects of gas breakout. The present study found that the gas uptake by the oil was highly dependent on the following factors; volumetric gas fraction, line pressure and liquid flowrate. The underlying water cut of the oil also appeared to have an effect.

## X-RAY VISUALISATION OF THREE-PHASE FLOWS

### INTRODUCTION

The X-ray visualisation system provides imaging of flow patterns through a section of pipe using the principle of simultaneous radiographic imaging in two orthogonal directions, using X-ray sensitive linear array detectors. The data from each linear array detector is read out at high speed to provide time-dependent information on different flow patterns.

The system can discriminate between all three phases (gas, water and oil). Dual energy X-ray data, combined with the use of a dopant (zinc sulphate) in the aqueous phase is needed to achieve adequate discrimination between the two liquid phases, which have similar X-ray attenuation characteristics. Facilities are also provided for imaging of any two of the three phases, using single-energy X-ray data. The key role of the system is to match one flow pattern against a previous one by visual comparison of the recorded data.

## DATA ACQUISITION & PROCESSING

### Computer System

The computer system consists of a desktop Pentium IBM-compatible PC, running Windows NT based software. The special-purpose software for the X-ray Visualisation system is accessed from a single icon within the Windows NT user-interface.

The block diagram in Figure 1 illustrates the key components of the computer system, and the interfaces with the overall system hardware.

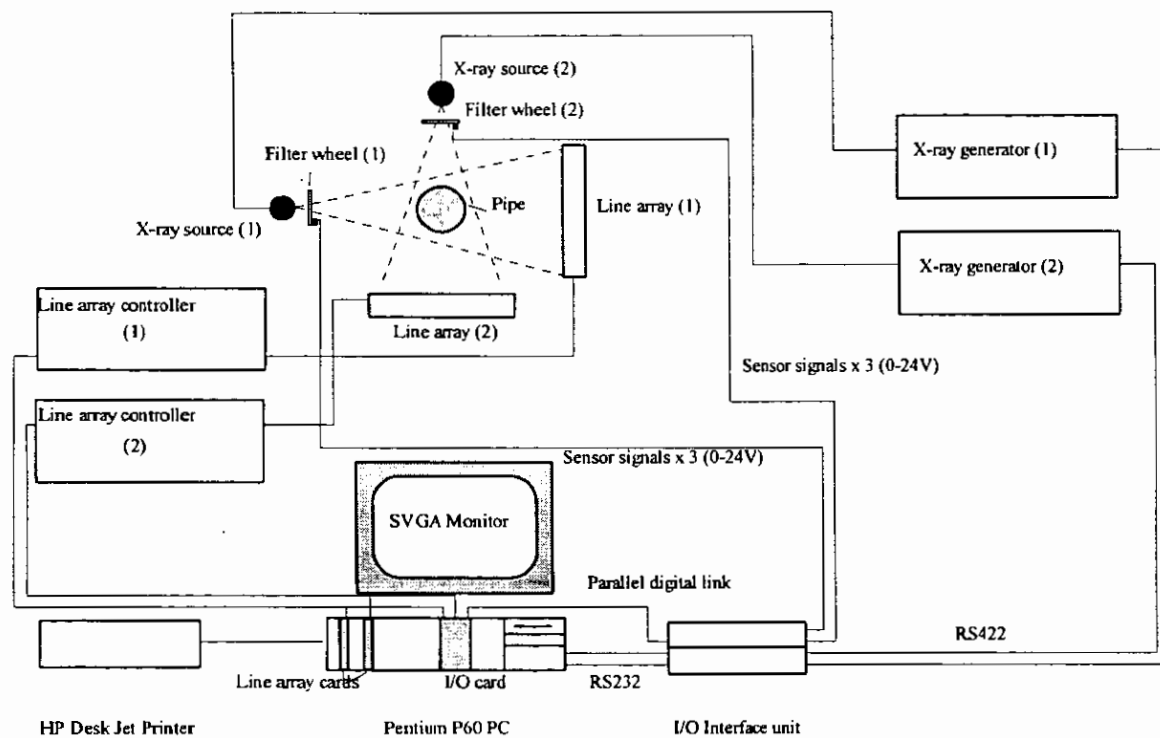


Figure 1: X-ray computer system block diagram

### Data Acquisition

The system is provided with two orthogonal line array detectors each with a separate X-ray generator. Figure 2 shows the locations of the two line arrays in relation to the external shape of the X-ray enclosure. Also shown in Figure 2 are the directions in which the data from the two arrays are plotted on the screen. The ends of the arrays marked Top/Right appear on the top of the images for a horizontal pipe and on the right-hand side of the images for a vertical pipe. Similarly, the ends marked

Bottom/Left appear on the bottom of the images and the left-hand side of the images for horizontal and vertical pipes respectively.

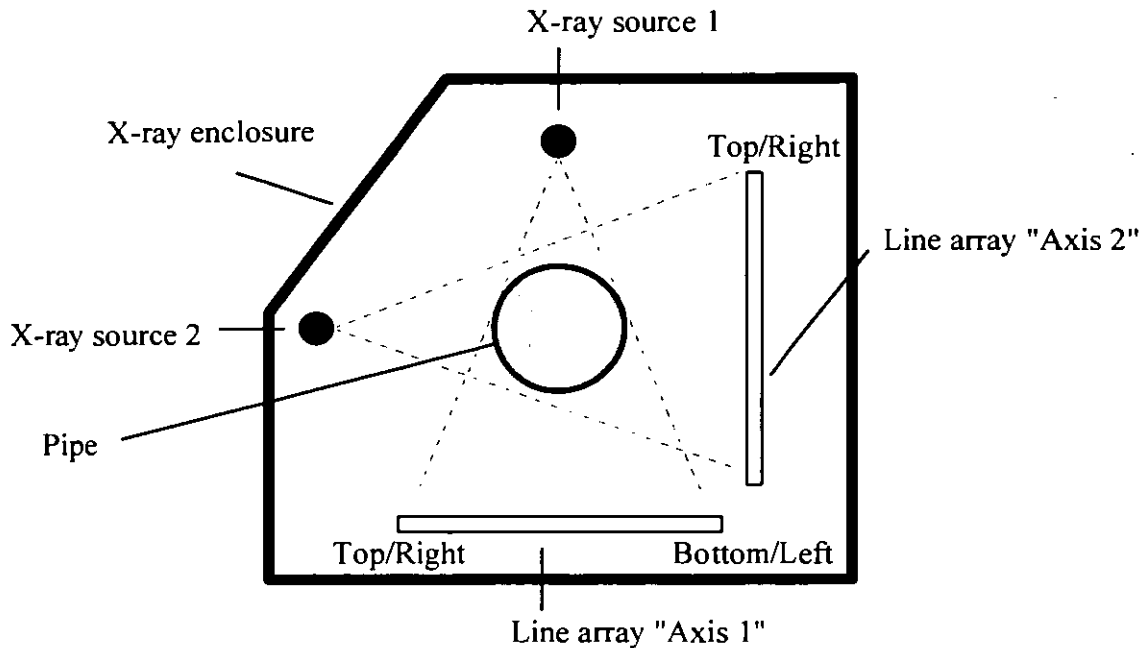


Figure 2: Arrangement of X-ray sources and detectors

In front of each X-ray generator is a rotating filter wheel, with three different sections (opaque lead, air and a sheet of copper). The rotation of the two wheels is synchronised, to prevent cross-talk between the two X-ray beams.

The copper and air sections of the rotating filter allow line array data to be collected at two different effective X-ray energies (hard and soft spectra, respectively) without the need to alter the X-ray supply voltage which could not be accomplished at the necessary speed. This allows three-phase (oil, gas and water) saturation information to be derived at high speed for both of the line arrays.

## Data Processing

### Time-dependent Radiographic Images

To obtain time-dependent radiographic (attenuation) images, the data from the line array is read out repeatedly, giving time-dependent information on the detected X-ray intensity at each pixel in the line array. This information is shown as a two-dimensional image in which one dimension of the image is the position across the line array, while the second dimension is time.

This allows a moving flow pattern to be visualised.

The data from the line array is presented in a number of different formats. The simplest shows the grey levels from the line array detector, which gives a radiographic image in which the image brightness is related to the intensity of the X-ray beam transmitted through the pipe.

### Time-dependent Saturation Images

The line array data can also be processed to produce two- and three-phase saturation information, as follows. For the single-energy line array data, two-phase information (i.e. the relative proportions of two different components, e.g. oil and water, along the line joining each pixel in the line array to the X-ray source) can be calculated. For the dual-energy line array data, three-phase information (i.e. the relative proportions of oil, water and gas) can be obtained.

To calculate saturation (or phase) information, it is necessary to have first recorded calibration information from the line array. This is obtained first by measuring the gain and offset of each line array independently, followed by a calibration of the two X-ray sets and line arrays with the pipe full of gas, oil and then water, with a slow speed rotation of the filter wheel mechanism.

It should be noted that the derivation of saturation information is complicated by the range of energies present in the soft and hard X-ray spectra. For dual-energy X-rays which are monochromatic at each energy, an exact mathematical solution is possible. However, for the continuous spectra of X-ray energies from the X-ray sources, no exact formula can be derived. Instead, the software uses an approximate method, based on an empirical correction method for the effects of "beam hardening". ("Beam hardening" is an effect which occurs due to the energy-dependent attenuation of the continuous X-ray spectra by the pipe contents - the lower X-ray energies are attenuated more than the higher energies, so that the average X-ray energy transmitted through a material increases with material thickness.)

The empirical correction method for the effects of beam hardening requires the use of two numerical parameters, the values of which have been fitted to the particular characteristics of the system. Numerical simulations suggest that the inherent accuracy of this method is typically about  $\pm 5\%$ , for the full three-phase calculations, in the absence of random noise on the data.

Thus, using the system the following three types of data can be displayed:

- Radiographic images (i.e. grey levels from line array detectors).
- Two-phase saturation information (relative proportions of phase 1 and phase 2).
- Full three-phase saturation information (relative proportions of oil, gas and water).

## RESULTS

### Horizontal flow

Figure 3 shows an example of imaging of a three-phase slug flow in a horizontal 4-inch pipe. The flowrates for this image were:

Water	0.279 m/s
Oil	0.196 m/s
Gas	2.26 m/s

The top figure (3a) shows the X-ray attenuation plot for the vertical and horizontal axes (axis 1 and axis 2 respectively). In this flow, separation of oil and water layers occurred between slugs and the oil can be seen clearly as a grey layer on top of the black layer representing the water. The thickness of the oil layer increases with time from the slug tail.

The lower figure (3b) shows the calculated saturation plots. The first two rows show the fraction of water, oil and gas as observed on the two axes, with white representing 100% and black 0% of a phase. The bottom row shows the effect of combining the two axes to give a cross-sectional image which is an average over the 2 minutes data recording period. This shows the water to be dominantly present at the base of the pipe, oil in the central layer and gas in the upper central region.

The software allows the averaging region to be focused in on any time interval to give the cross-sectional information resolved to more detail.

### Vertical flow

Figure 4 shows an example of imaging of a three-phase slug flow in a vertical 4-inch pipe. The flowrates for this image were:

Water	0.728 m/s
Oil	0.258 m/s
Gas	1.96 m/s

Again the top figure (4a) shows the X-ray attenuation data and the bottom figure (4b) the saturation data. In this flow condition, the flow observed consisted of 'plugs' of liquid alternating with a long gas bubble / churning region. The liquid plugs correspond to the dark regions on the attenuation plot and the churn regions to the greyer areas.

The oil and water were well-mixed and this is shown on the saturation plots (this type of saturation plot is very typical of those observed in vertical flows). The right hand column in figure 4(b) shows the cross-sectional averages of water, oil and gas fractions, which indicate a very low average liquid fraction and a large gas core. (The

eccentric position of the gas core resulted from a slight misalignment of the X-ray instrument with the vertical test section).

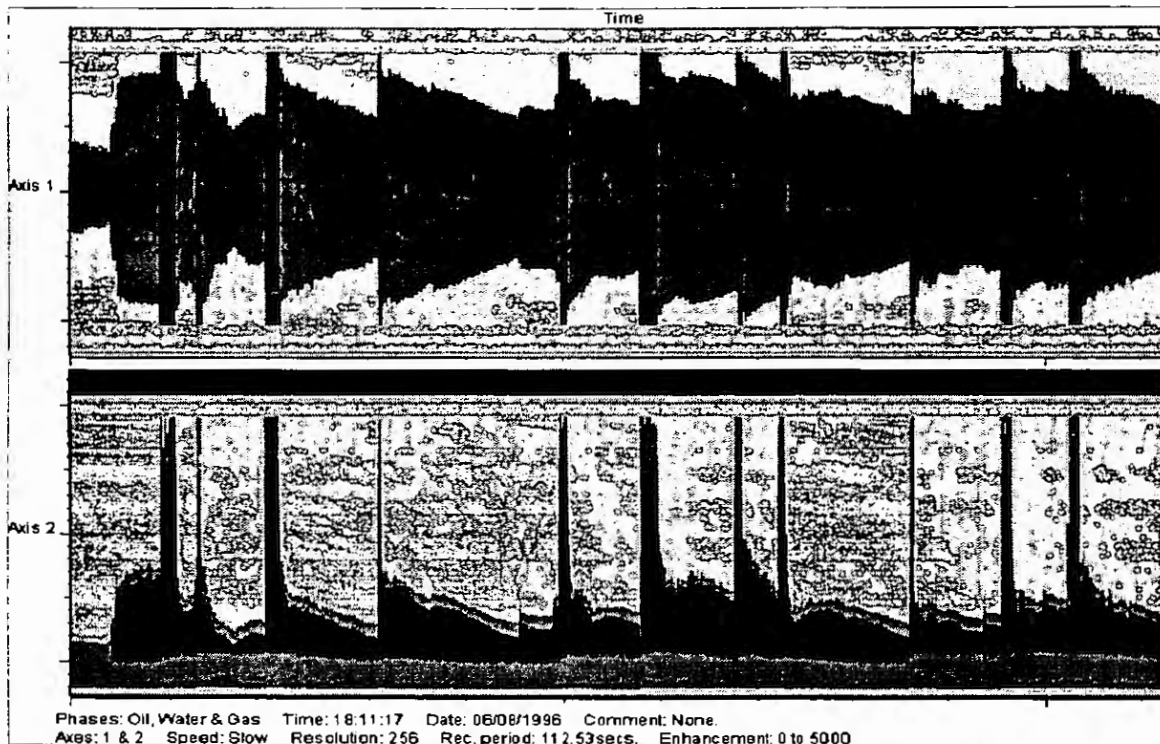


Figure 3(a): X-ray attenuation plot for horizontal 3-phase slug flow

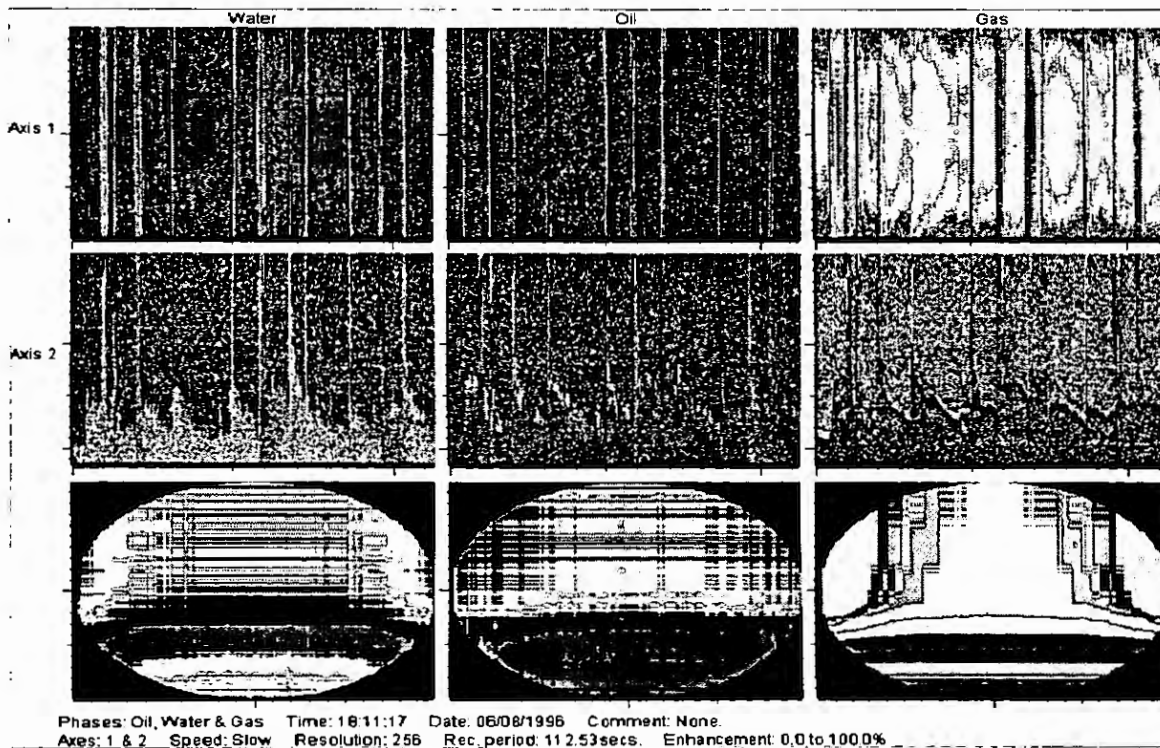


Figure 3(b): X-ray saturation plot for horizontal 3-phase slug flow

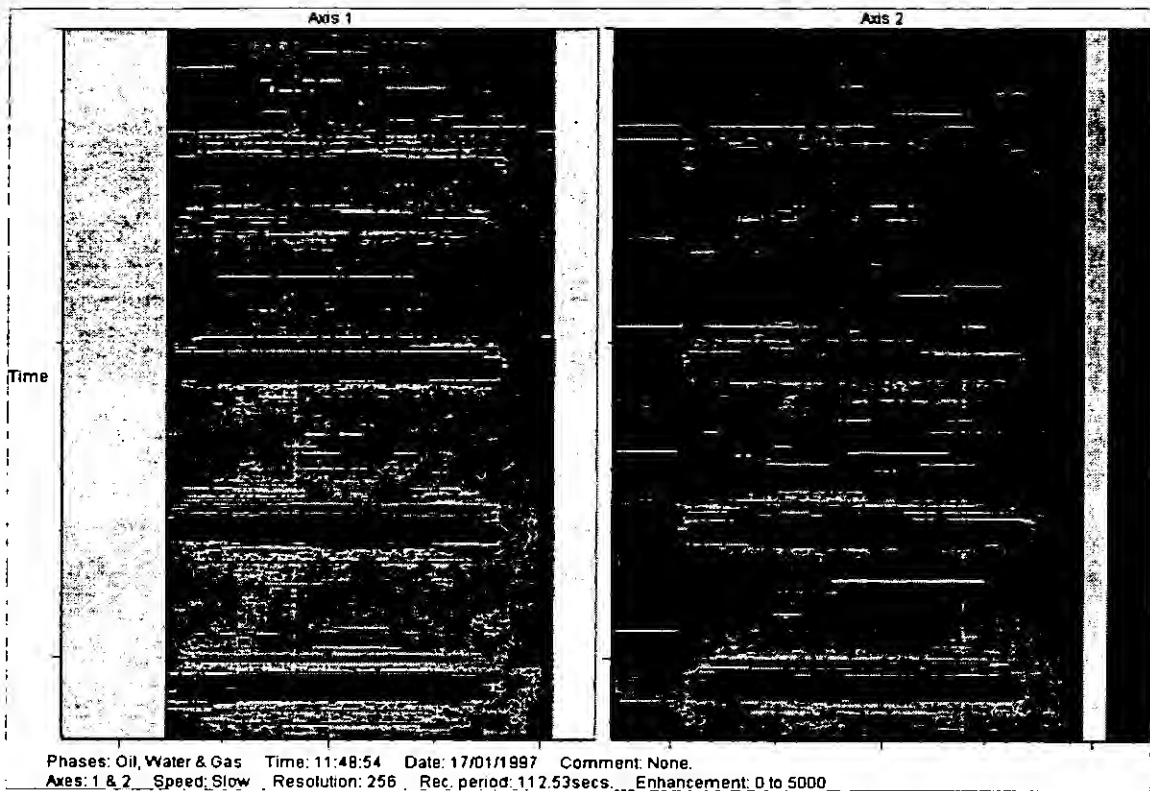


Figure 4(a): X-ray attenuation plot for vertical 3-phase slug flow

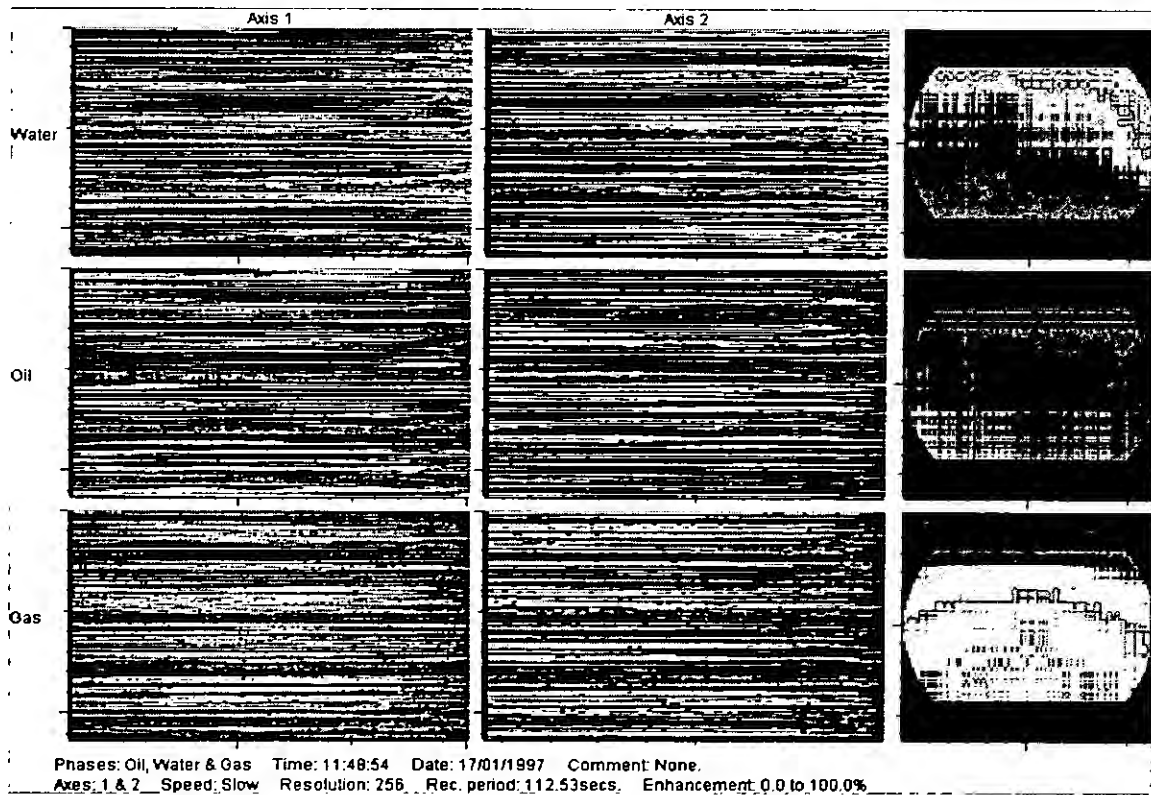


Figure 4(b): X-ray saturation plot for vertical 3-phase slug flow



# DISSOLVED GAS QUANTIFICATION

## INTRODUCTION

The principle of this study is that the solubility of a gas in a liquid is proportional to the absolute pressure. If a sample of liquid is subjected to a vacuum, the entrained gas is released and so can be measured. The method used to facilitate this measurement is a modification of that of Hayward [1], in which an oil sample was expanded and then compressed. The present method employs a dual expansion technique.

Experiments were performed at a constant pressure of 5 bar and with a mixture of crude oil and nitrogen. The gas volume fraction was changed to investigate the effect of this parameter on the gas absorption of the oil. The volume fractions at which the data points were taken were repeated using oil with a higher water content. Further data points were taken at lower pressures in order to analyse any effects due to a change in line pressure. Static experiments were performed also in which oil was poured directly into the sampler.

## THEORY

The gas content of a liquid,  $\alpha$ , is defined as

$$\alpha = \frac{100 V_{gas}(T_{STP}, P_{STP})}{V_{liq}} \quad (1)$$

where  $V_{gas}(T_{STP}, P_{STP})$  is the volume of gas evolved at standard temperature and pressure,  $T_{STP}$  and  $P_{STP}$  are the absolute temperature and pressure corresponding to conditions of standard temperature and pressure, 273.15 K and 101325 Pa respectively and  $V_{liquid}$  is the volume of the liquid sample. If a dual expansion procedure is executed, using Henry's Law, the value of  $\alpha$  can be calculated as follows,

$$\alpha = 100 \frac{[(p_1 - p_2)/P_{STP}] (T_{STP}/T) \{ [V_1 + V_{ptr}(T/T_{ptr})]/V_{liq} \} (1 + P_{gas2}/P_{line})}{\{ -n - [(P_{gas1} - nP_{gas2})/P_{line}] \}} \quad (2)$$

where

- $p_i$ : pressure after  $i$ th expansion
- $P_{line}$ : line pressure
- $P_{gasi}$ :  $P_i - P_{vac}$
- $P_{vac}$ : pressure after manometric system has been evacuated
- $n$ : expansion ratio from first to second deaeration chambers
- $V_1$ : volume of first deaeration chamber and associated pipework
- $V_2$ : volume of second chamber and associated pipework
- $V_{ptr}$ : volume of pressure transducer

$T$ : ambient temperature  
 $T_{ptr}$ : temperature of pressure transducer

## METHOD

Figure 5 shows the apparatus used to perform the present experiments. It consists of a sampling system to remove a known volume of liquid, free of gas bubbles, from the flowline and a manometer system to perform the dual expansion. In the figure, valves are labelled as 1 to 5 and A and B are the expansion cylinders. The apparatus was positioned in the multiphase loop at NEL, approximately 25 m downstream of the gas injection point.

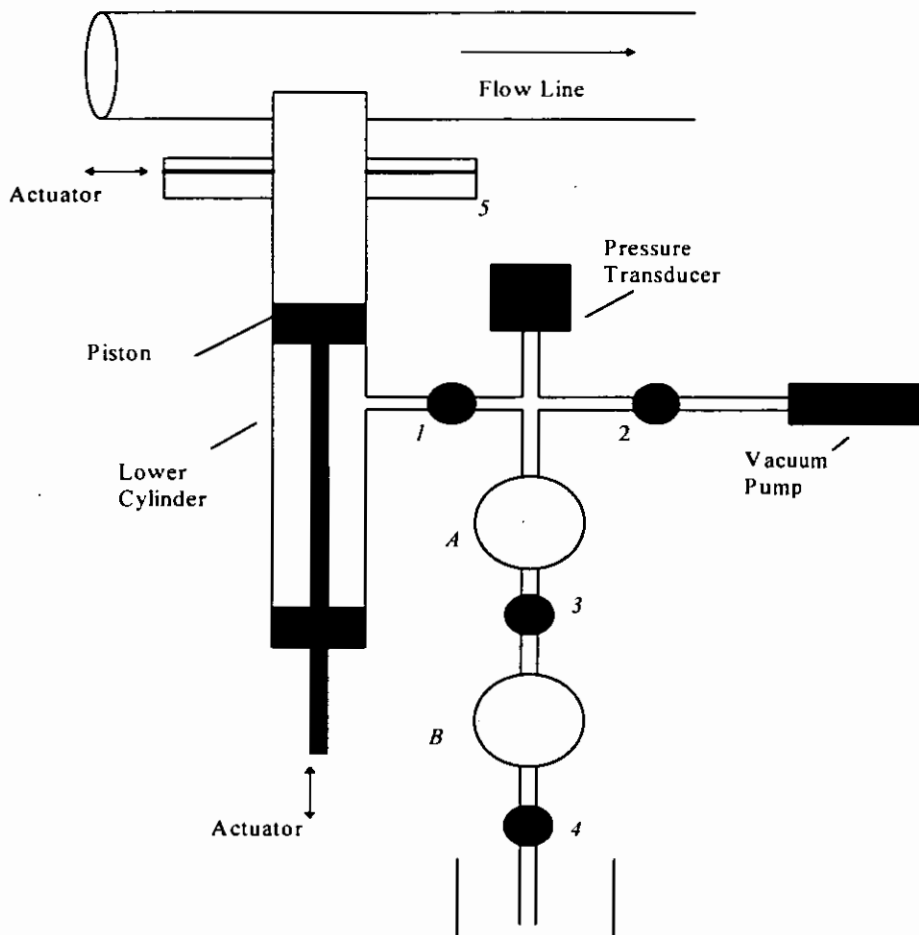


Figure 5: Schematic diagram of sampling and manometric systems

Prior to sampling, valve 1 is shut and the manometer evacuated. To take a sample, valve 5 is opened and the piston slowly lowered. It is essential that the sample is withdrawn slowly, in the order of 30 s, to ensure that bubbles are not drawn far below the neck of the tube. Valve 5 is then shut and valve 1 opened to allow expansion in to the first cylinder. Once the pressure is stable, valve 3 is opened and the liquid is

expanded in to the cylinder B. Three observations of pressure, that of the initial vacuum and after both expansions, together with the ambient air temperature reading are used to calculate the gas content  $\alpha$  as described in the previous section.

Initial results indicated that the system design is such that a time of greater than ten hours is necessary for the first expansion. However, the majority of the gas appears to come out of solution within an hour of the second expansion. Hence the sample was left overnight for the first expansion process and an hour for the second.

## RESULTS

### Variation of $\alpha$ with Gas Volume Fraction

The gas content of the oil is highly dependent on the gas volume fraction (G.V.F) of the flow.

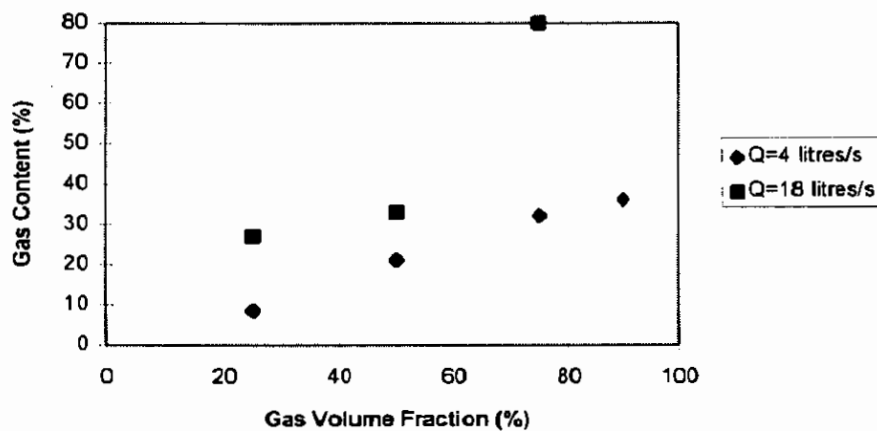


Figure 6: Variation of  $\alpha$  with gas volume fraction at 3% water cut

Figure 6 shows that in an oil with a low water cut (3%), the value of  $\alpha$  increases as the percentage of gas within the flow increases. This occurs at both the liquid flowrates investigated. It is also clear that for a given gas volume fraction (G.V.F),  $\alpha$  increases if the liquid flowrate is increased from 4 litres/s to 18 litres/s.

If the water content of the oil is increased, although the general trend of increasing gas content with G.V.F is continued, the value of  $\alpha$  at a particular gas volume is decreased. This can be seen in Figure 7. For example, at a G.V.F value of 90%,  $\alpha$  has a value of 19% as compared with 36% in Figure 6. The flowrates within this figure are 3-4 litres/s.

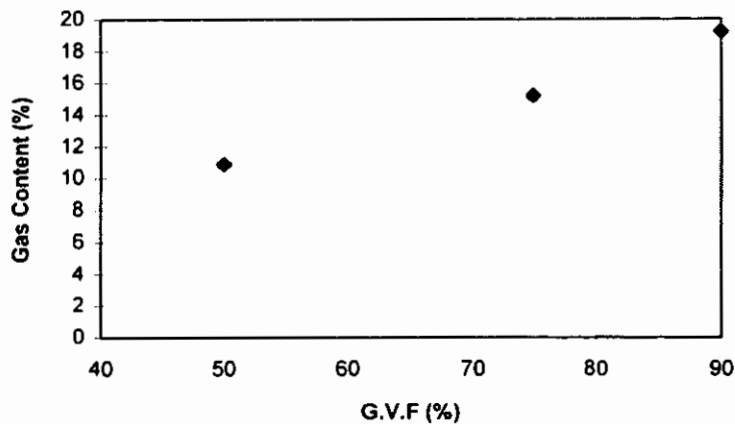


Figure 7: Variation of  $\alpha$  with gas volume fraction at 12% water cut

### Variation of Gas Content with Line Pressure

Three experiments which were performed at a line pressure lower than 5 bar. The results are shown in Table 1. The flowrates for this data were between 4 and 6 litres/s and the water cut was 3% for the points at 2 bar and 6% at 0.6 bar.

Table 1: Effect of line pressure on the gas content of the oil

$P_{line}$ (bar)	G.V.F (%)	$\alpha$ (%)
0.6	95	9.0
2	90	13.4
2	75	4.3

Although the gas volume fraction for the point taken at 0.6 bar is slightly higher than that at 2 bar, there is a considerable difference in the value of  $\alpha$  which is larger than the estimated uncertainty (approximately 6%). The value at 2 bar is lower than that found at 5 bar. When the gas volume fraction is decreased, the value of  $\alpha$  decreases also, consistent with previous trends, but the value itself is lower than that at 5 bar. This indicates that line pressure significantly affects the gas absorption by the oil; the greater the line pressure, the higher the gas content of the oil.

### Static Tests

Samples of crude oil were left in trays to become saturated with air. This technique was found by Hayward [2] to be the easiest method for air absorption. Two samples of oil were used in these tests, one had been left for several weeks (Oil I) and the other for two days (Oil II). The oils were then poured into the top of the sampling tube, the ball valve shut and the rest of the experimental procedure continued. The corresponding values of gas content for these two oils are as follows

**Oil I:**  $\alpha = 3.5 \%$

**Oil II:**  $\alpha = 2.3 \%$

The difference in the two values may be either the result of experimental error or that two days was insufficient for the oil to become fully saturated with air. These values do not correspond to those found by Hayward [2] for a variety of air saturated oils. He found that, on average,  $\alpha$  had a value of 8 % at atmospheric pressure. A possible reason for this disparity is that the depth of the tray in the present experiments may have been too large for the bulk of the oil to become saturated with air. Thus the above values of  $\alpha$  may correspond to oil with only surface saturation.

## **CONCLUSIONS**

### **X-ray Visualisation**

Imaging of three-phase flows using X-ray attenuations has been successfully demonstrated using this system. The flow structure can be resolved in some considerable detail, with the greatest success in horizontal flows.

### **Gas Quantification**

A dual expansion volumetric/manometric system can be used to calculate the dissolved gas content of a hydrocarbon oil. The value of dissolved gas content,  $\alpha$ , increases as the gas volume fraction increases. Results also indicate that  $\alpha$  depends on the line pressure at which the tests are conducted and the background water content of the oil.

## **ACKNOWLEDGEMENTS**

The work described in this paper was funded by the Flow Programme of the UK Department of Trade & Industry.

## **REFERENCES**

1. HAYWARD, A.T.J., "Two new instruments for measuring the air content of oil", *Journal of the Institute of Petroleum*, 47(447), 99 - 106, 1961
2. HAYWARD, A.T.J., "The air-solubility of hydraulic oils", NEL Report 53, 1962